Prace Naukowe Instytutu Maszyn, Napędów i Pomiarów Elektrycznych
Nr 65 Politechniki Wrocławskiej Nr 65

Studia i Materiały Nr 31 2011

induction motor, Direct Torque Control,
field weakening, optimal control

Khanh NGUYEN THAC*
Teresa ORŁOWSKA-KOWALSKA*

COMPARATIVE ANALYSIS OF CHOSEN FIELD WEAKENING METHODS FOR THE SPACE VECTOR MODULATED – DIRECT TORQUE CONTROLLED DRIVE SYSTEM

This paper presents a new simple field weakening (FW) strategy for the Direct Torque Control (DTC) of the induction motor (IM). Based on the Space Vector Modulated–Direct Torque Control (SVM-DTC) scheme, an analysis and comparison of conventional ($1/\omega_m$) and proposed method are presented for a whole speed range including FW regions. The proposed strategy is verified through simulation with a 1.5 kW induction motor drive.

1. INTRODUCTION

Many methods of controlling the performance of the induction motor (IM) exist, but mainly Field Oriented Control (FOC) and Direct Torque Control (DTC) deserve special attention as both techniques can be considered as high performance vector controllers based on the decoupling of motor flux and torque. The DTC systems, which were first introduced in the mid 1980s, achieved a very quick and precise torque control response without necessity of complex algorithms usage. [6], [15].

Recently, from the classical DTC methods, some new control techniques have been developed. The overview of the DTC methods was presented in [1]. According to those DTC methods, some schemes were applied for controlled IM drives in the field weakening (FW) region.

Based on the switching table – DTC method (ST-DTC), robust schemes for wide speed range of FW are proposed in [3]–[5]. In these schemes authors presented FW

* Institute of Electrical Machines, Drives and Measurements, Wroclaw University of Technology, ul. Smoluchowskiego 19, 50-372 Wroclaw, Poland; e-mail: khanh.nguyen.thac@pwr.wroc.pl, teresa.orlowska-kowalska@pwr.wroc.pl

algorithm with on-line estimation of the break-down torque. Simple structure and very good dynamic behavior are main features of classical ST-DTC based schemes. However, classical DTC has several disadvantages, from which the most important is variable switching frequency.

In the paper [10] another algorithm for the IM torque control in FW region is presented. Proposed method insures maximum DC bus utilization and offers DTC performance through the stator voltage angle control.

Taking into account a voltage limit ($u_s \le U_{\max}$) and a current limit ($i_s \le I_{\max}$) of inverter and IM in FW region, in [11] a control strategy for FW-operation-based DTC method with maximum torque capability algorithm was presented. The control scheme utilizes the stator flux components as control variables and decreases the d-component of the stator flux as soon as the voltage corresponding to the maximum torque achievable at a given speed tends to exceed the maximum voltage.

Direct flux vector control strategy was suggested in [8], [16] - [19] based on a simple method for the IM control – Direct Torque Control with Flux Vector Modulation (FVM-DTC). In these schemes, the calculation of reference voltage vector is based on demanded stator flux vector error, $\Delta\boldsymbol{\psi}_s = \boldsymbol{\psi}_s^* - \hat{\boldsymbol{\psi}}_s$ (where $\boldsymbol{\psi}_s^*, \hat{\boldsymbol{\psi}}_s$, are reference and estimate of stator flux vectors). However this control strategy is very sensitive to disturbances, because of differentiation algorithm. In case of errors in the feedback signals, the differentiation algorithm may not be stable. This is very serious drawback of those methods [20].

Recently, from the classical DTC methods a new control technique, called Space Vector Modulated – Direct Torque Control (SVM-DTC), has been developed and improved. The SVM-DTC method has been described and deeply analyzed in [20]. In this method disadvantages of the classical DTC are eliminated. Basically, the SVM-DTC strategies are the methods, which operate with constant switching frequency. Moreover, the SVM-DTC has best performances, but it requires more complex control scheme and the knowledge of some IM parameters [9], [14].

In this paper, a modified SVM-DTC scheme with optimal FW of the IM drive in whole speed range is proposed. The performance of this structure under such control is compared to that obtained using classical $1/\omega_m$ FW control strategy.

2. OPERATION MODES OF THE INDUCTION MOTOR IN CURRENT AND VOLTAGE LIMIT CONDITION

The operating speed range of the IM drive can be divided in three sub-regions: constant torque region ($\omega_s < \omega_{sb}$), constant power region ($\omega_{sb} \le \omega_s < \omega_{sc}$) and constant slip frequency region ($\omega_s \ge \omega_{sc}$) [7], as is shown in Fig. 1 (where ω_{sb}, ω_{sc} are base and critical stator angular speeds).

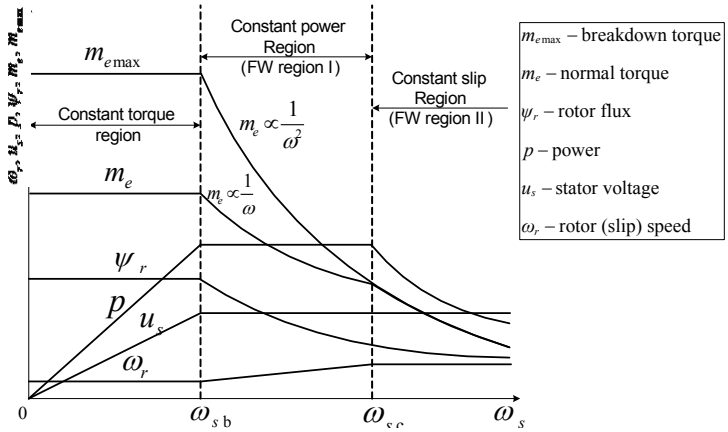

Fig. 1. Control characteristics of the induction motor in constant and weakened flux regions

The maximum torque of the induction motor is limited by the current and voltage ratings of the power inverter and thermal current limit of the IM. Therefore, it is useful to analyze the machine's performance under the current and voltage constraints in the $x-y$ synchronous reference frame, rotating with the angular frequency $\omega_s = \omega_{s\psi}$.

The current constraint of the inverter can be expressed as follows:

$$i_{sx}^2 + i_{sy}^2 \le I_{\max}^2 \tag{1}$$

where: $I_{\max}^2 = |\mathbf{i}_s| = \sqrt{i_{sx}^2 + i_{sy}^2}$ – the maximum stator current magnitude, i_{sx}, i_{sy} – stator current vector components of the IM in the field-oriented $x-y$ coordinate system [p.u.]. This relationship limits the current magnitude to the circle defined by $I_{\max}$.

The voltage constraint of the inverter is given as:

$$s_{sx}^2 + u_{sy}^2 \le U_{\max}^2 \tag{2}$$

where: u_{sx}, u_{sy}, $U_{\max}$ – components of the stator voltage vector in $x-y$ coordinates and the maximum voltage magnitude [p.u.], respectively.

$U_{\max}$ is set by the available voltage, which is function of the pulse-width-modulation strategy and the available DC-bus voltage (U_{dc}). This equation indicates that the voltage magnitude $|\mathbf{u}_s| = \sqrt{u_{sx}^2 + u_{sy}^2}$ cannot exceed the ellipse defined by $U_{\max}$. Nowadays mainly the Space Vector Modulation (SVPWM) is used, thus the $U_{\max}$ is limited to $U_{dc}/\sqrt{3}$.

The steady-state stator voltage equations of the IM under rotor field oriented frame (in [p.u.]) are given directly from the motor mathematical model [13]:

$$u_{sx} = r_s i_{sx} - \omega_s \sigma x_s i_{sy} \tag{3a}$$

$$u_{sy} = r_s i_{sy} - \omega_s x_s i_{sx} \tag{3b}$$

where: r_s, r_r – stator and rotor winding resistance, x_s, x_r – stator and rotor winding self-reactance, x_M – induction motor main reactance, $\sigma = 1 - x_M^2 / x_s x_r$ – total leakage factor.

The equation for the voltage limit ellipse (4a) and current limit ellipse (4b) can be derived by substituting (3a), (3b) into (2) and (1):

$$\left(\frac{r_s i_{sy}}{U_{\max}} + \frac{x_s i_{sx}}{U_{\max}/\omega_s}\right)^2 + \left(\frac{r_s i_{sx}}{U_{\max}} - \frac{\sigma x_s i_{sy}}{U_{\max}/\omega_s}\right)^2 \le 1 \tag{4a}$$

$$\left(\frac{r_s u_{sx} + \omega_s \sigma x_s u_{sy}}{I_{\max}(r_s^2 + \omega_s^2 \sigma x_s^2)}\right)^2 + \left(\frac{r_s u_{sy} - \omega_s x_s u_{sx}}{I_{\max}(r_s^2 + \omega_s^2 \sigma x_s^2)}\right)^2 \le 1 \tag{4b}$$

In the case of rotor flux oriented control of the IM, the rotor flux, $\boldsymbol{\psi} = \boldsymbol{\psi}_r = \psi_{rx} = x_M i_{sx}$, and electromagnetic torque can be described as follows [13]:

$$m_e = \frac{x_M}{x_r}\psi_r i_{sy} = \frac{x_M^2}{x_r} i_{sx} i_{sy} \xrightarrow[r_s \text{ is neglected}]{\text{(3a), (3b)}} m_e = -\frac{x_M^2}{\sigma x_r x_s^2}\frac{u_{sx}}{\omega_s}\frac{u_{sy}}{\omega_s} \tag{5}$$

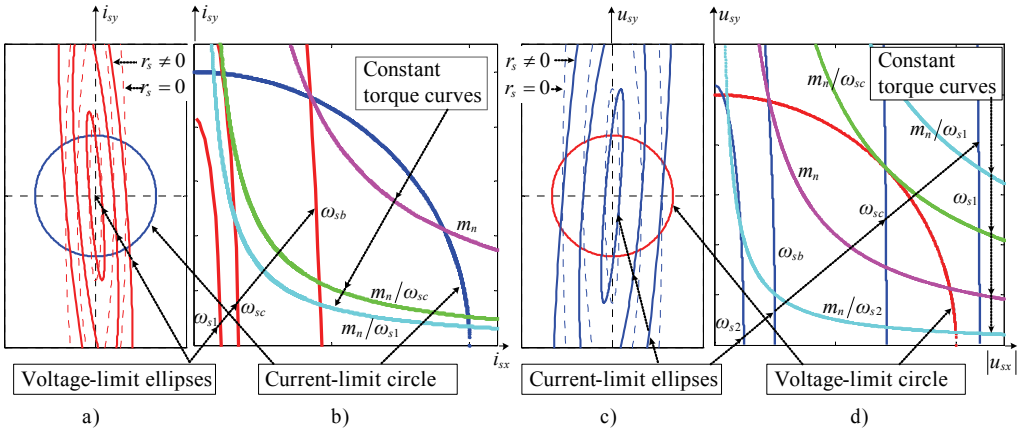

Fig. 2. a) Current-limit circle (1) and voltage-limit ellipse (4a); c) voltage-limit circle (2) and current-limit ellipse (4b); b, d) details of Fig. 2a,c with data of the investigated induction motor

Basing on those expressions the current-limit circle and voltage-limit ellipses (with radiuses are reduced when speed is increased – according to (4a)) are shown in Fig. 2a, b; the voltage-limit circle and current-limit ellipses (with radiuses are enlarged when speed is increased – according to (4b)) are shown in Fig. 2c, d. The dotted line ellipses in Fig. 2a, c are forms the constraints when the stator resistance is neglected. In contrast,

the bold line ellipses are the constraints when the stator resistance is included. The stator resistance is affecting the operating conditions of the IM at low speeds region and can be neglected in high-speed region.

3. FIELD WEAKENING ALGORITHMS

The field-weakening algorithm applied in DTC structure should provide robust and stable torque regulation in whole speed range including FW region, by making sure that the IM is operated within the voltage and the current maximum constraints. Under the assumption of the slow enough variation of the rotor flux and the precise vector control, the currents and voltages maximizing the torque (5) of the IM, can be derived from the constraints given by (1), (2) and (4). The possible operating region is inside the area of the voltage circle and current ellipse and the torque is depicted as a reciprocal proportion curve in the voltage plane, as shown in Fig. 2c, d.

3.1. CONSTANT TORQUE REGION ($\omega_s \le \omega_{sb}$)

In the SVM-DTC the voltage components u_{sx}, u_{sy} should be controlled. In the normal speed (constant torque) region, the magnitude of the voltage vector $\mathbf{u}_s^* = u_{sx}^* + ju_{sy}^*$, which regulates the rated x and y voltage components (u_{sx}, u_{sy}) is always less than $U_{\max}$. As a result, for maximum torque generation, in this region the operating point should lie on the AB line, inside the voltage-limit circle, as in Fig. 3 – that are intersection points (×) between current-ellipses and rated torque curves (at the same speed).

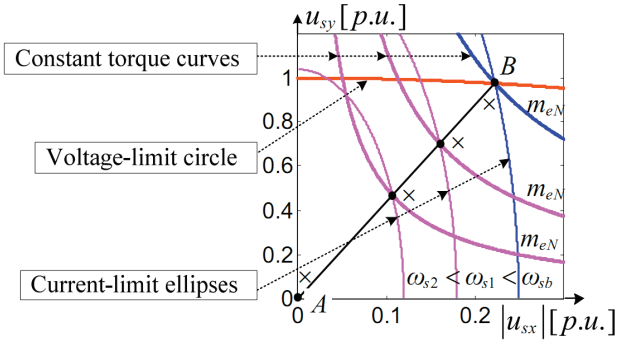

Fig. 3. Constant torque region for voltage-based control method

According to (5), to keep constant torque, maximum values (limits) of the reference voltage components can be obtained as:

$$\begin{cases} u^*_{sx\,\mathrm{lim}}\big|_{\text{constant torque}} = \omega^*_s u_{sxb} / \omega_{sb} \\ u^*_{sy\,\mathrm{lim}}\big|_{\text{constant torque}} = \omega^*_s u_{syb} / \omega_{sb} \end{cases} \tag{6}$$

where u_{sxb} and u_{syb} (co-ordinate of B point) can be obtained from (9) with $\omega_s = \omega_{sb}$.

The angular frequency, where the constant torque operation region ends, is defined as the stator base frequency, ω_{sb} (at point B in Fig. 3), and neglecting the stator resistance; it can be obtained from (4a) as follows:

$$\omega_{sb} = U_{\max} / (x_s \sqrt{i^2_{sxN}(1-\sigma^2) + \sigma^2 I^2_{\max}}) \tag{7}$$

3.2. CONSTANT POWER REGION ($\omega_{sb} \le \omega_s < \omega_{sc}$) – FIELD WEAKENING REGION I

In this operation region of the IM, delivering the rated power, the torque production will be inversely proportionally to the speed:

$$m_e \propto \frac{1}{\omega_m} \cong \frac{1}{\omega_s} \tag{8}$$

This operation region starts from the base speed, ω_{sb}, and ends at a critical speed, ω_{sc}, above which there is no more crossing point between the ellipse (at ω^*_s) and the constant torque curve (at command torque value $m^*_e = m_{eN} / \omega^*_s$), see in Fig. 4).

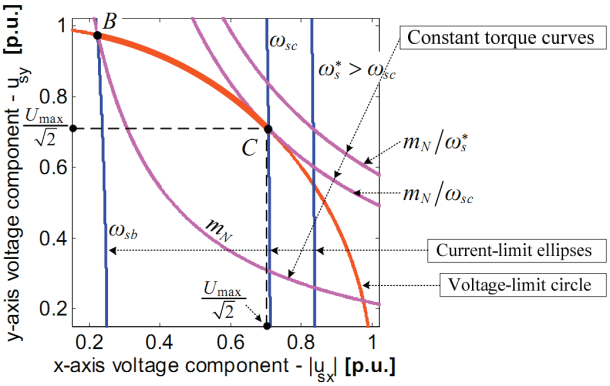

Fig. 4. Field weakening region I in voltage coordinates plane

In Figure 4, to obtain maximum torque in FW region I, the voltage vector must slide on line BC, which is intersection between the voltage limit circle, the current limit ellipse and the constant torque curve. When $\omega_s = \omega_{sc}$, the voltage limit circle and the con-

stant torque curve (at $m_e = m_{eN} / \omega_s^*$) intersect each other at only one point (contact point *C*) – see in Fig. 4.

The limit of reference voltage can be obtained when equating (2) and (4b):

$$\begin{cases} \left|u_{sx\,\mathrm{lim}}^*\right|_{\text{constant power}} = \sigma\sqrt{\omega_s^2 x_s^2 I_{\max}^2 - U_{\max}^2} \,/\, \sqrt{1-\sigma^2} \\ u_{sy\,\mathrm{lim}}^*\Big|_{\text{constant power}} = \sqrt{U_{\max}^2} - (u_{sx\,\mathrm{lim}}^*)^2 \end{cases} \tag{9}$$

In this region, the slip angular frequency is increased as the speed increases. As the speed is further increased, the slip reaches the maximum value due to the voltage limit and then the II FW region begins. The slip speed value for maximum torque is given by the following expression [7]:

$$\omega_{r\max} = r_r\sqrt{\omega_s^2 x_s^2 + r_s^2} \,/\, \sqrt{(\sigma\omega_s x_r x_s)^2 + r_s^2 x_r^2} \tag{10}$$

3.3. CONSTANT SLIP REGION ($\omega_s \geq \omega_{sc}$) – FIELD WEAKENING REGION II

As the slip angular frequency and the speed are further increased, the stator operating frequency is increased, and also thus the current ellipse is more increased, so its large portion begins to be outside the voltage circle shown in Fig. 5.

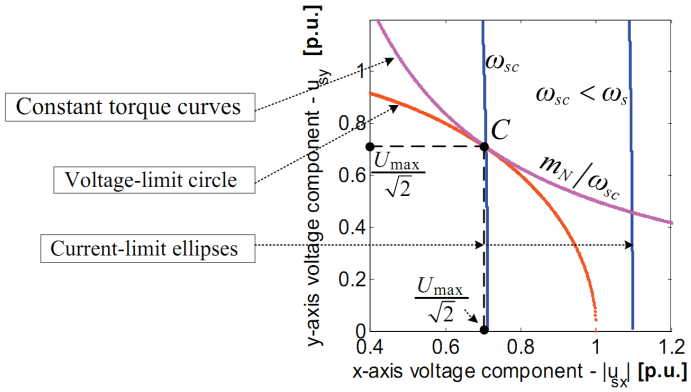

Fig. 5. Field weakening region II for voltage coordinates plane

The onset of region II ω_s is time, when for the optimal voltage values for given maximum torque, only the current limits is the constraint to be considered. The steady-state electrical torque is proportional to $u_{sx}u_{sy}$ (5). Meantime, $\mathbf{u}_s = U_{\max}e^{j\varphi}$ so $u_{sx}u_{sy} = \frac{1}{2}U_{\max}^2 \sin 2\varphi$. Thus, the torque is maximized if $\sin 2\varphi = 1$, i.e.,

$|u_{sx}| = |u_{sy}| = U_{\max}/\sqrt{2}$ (point C in Fig. 5). Therefore, the optimal voltage components for the maximum torque can be obtained as (11)

$$\left|u_{sx\lim}\right\|_{\text{constant slip}} = \left|u^*_{sy\lim}\right\|_{\text{constant slip}} = U_{\max}/\sqrt{2} \tag{11}$$

Figure 5 shows the trajectory for maximum torque in FW region II, that is point *C* in the voltage coordinates plane.

Assumed that stator resistance is neglected, substituting (11), into (3) and (1) we obtain stator critical speed, ω_{sc} as (12):

$$\omega_{sc} = U_{\max}\sqrt{2(\sigma^2+1)}/(2\sigma x_s I_{\max}) \tag{12}$$

Limit of torque regulator ($m_{.e\lim}$) can be obtained from (5) with u_{sx} and u_{sy} are replaced by $u^*_{sx\lim}$ and $u^*_{sy\lim}$ as $\left|m^*_{e\lim}\right| = (x_M^2 u^*_{sx\lim} u^*_{sy\lim})/(\sigma x_r x_s^2 \omega_s^{*2})$.

3.4. THE CLASSICAL "$1/\omega_m$" METHOD

For the FW operation, a commonly used method is to vary the reference flux inversely proportional to the mechanical speed ω_m [18]. According to (3), if stator resistance is neglected, the flux and torque current components can be obtained as:

$$\begin{cases} i^*_{sx} = u^*_{sy}/(\omega_s x_s) \\ i^*_{sy} = -u^*_{sx}/(\omega_s x_s \sigma) \end{cases} \tag{13}$$

In the classical method, the reference voltage u^*_{sx} and u^*_{sy} are not limited by constraint conditions ($U_{\max}$ and $I_{\max}$). As a result, the current components in (13) are not limited by constraint conditions too.

As a result, the voltage margin enough to regulate the current reference cannot be maintained. Thus, in a high speed region (FW region I) the IM operation may be unstable depending on the machine parameters. In a very high speed region (FW region II), this method does not guarantee the condition (11), and the drive system is operated in an unstable torque region. As a result, the current control falls and the drive system losses its controllability.

3.5. REFERENCE STATOR FLUX

In the DTC methods, we should use the stator flux reference ψ^*_s instead ψ^*_r (as in DFOC method [12]). Supposing that the reference rotor flux ψ^*_r is known, the stator flux reference can be calculated based on the steady-state IM model as [1], [2]:

$$\psi_s^* = \sqrt{\left(\frac{x_s}{x_M}\psi_r^*\right)^2 + (\sigma x_s)^2\left(\frac{x_r}{x_M}\frac{m_e^*}{\psi_r^*}\right)^2} \tag{14}$$

In the classical DTC method we can calculate the ψ_s^* by a simple way as (15) [13], based on the nominal torque and rotor slip pulsation for constant flux region:

$$\psi_{s\,\text{classical}}^* = \begin{cases} \psi_{sN}\sqrt{m_{eN}\left[\left(\frac{r_r}{\sigma x_r}\right)^2 + \omega_{rN}^2\right] \Big/ \left[\left(\frac{x_M}{\sigma x_s x_r}\right)^2 r_r \omega_{rN}\right]} & \text{if } \omega_m \le \omega_{mb} \\ \frac{\psi_{sN}}{\omega_m} & \text{if } \omega_m > \omega_{mb} \end{cases} \tag{15}$$

4. CONTROL SYSTEMS IMPLEMENTATION

Figure 6 shows the block diagram of the SVM-DTC structure for the IM drive system, including possibility of switching between classical FW ($1/\omega_m$) and optimal FW methods. The control structure system consists of the speed, torque, flux PI regulators and current-voltage simulator for estimation of the electromagnetic torque and stator flux vector.

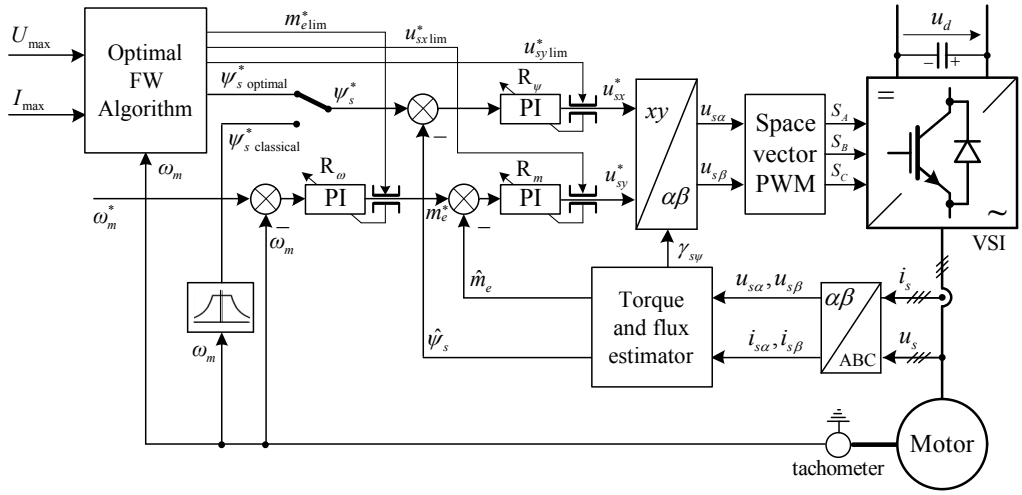

Fig. 6. Block diagram of the SVM-DTC

Figure 7 shows the block diagram of the optimal field-weakening algorithm based DTC method, developed in Section 3.

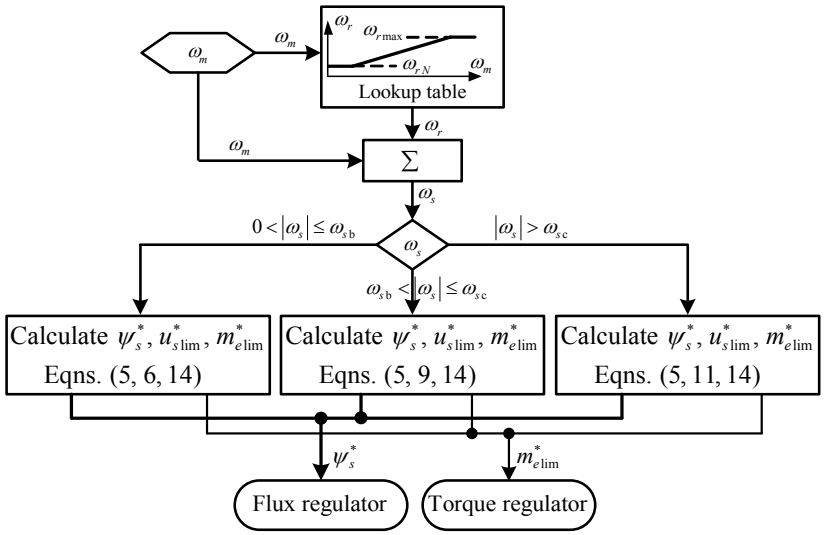

Fig. 7. Block diagram of the optimal FW algorithm for SVM-DTC method

5. SIMULATION RESULTS

In the following figures chosen simulation results for tests of both flux weakening algorithms are presented and compared (with 3.0 kW, 1400 rpm induction motor and following per-unit parameters: r_s = 0.0707, r_r = 0.0637, $x_s = x_r$ = 1.9761, x_M = 1.8780, ψ_{rN} = 0.8. Simulations were performed for the same voltage and current limit constraints ($I_{\max}$ = 1.5 [p.u.], $U_{\max}$ = 1.0 [p.u.]), thus the value of the base and critical speeds were obtained as ω_{sb} = 1.029 [p.u.] and ω_{sc} = 2.5 [p.u.]. For each test, two FW methods used the same load torque and reference speed characters.

In Figure 8 simulation results under no load and linear speed reference ramp start-up and steady state at ω_m = 3.0 [p.u.] speed are shown. It is seen that in the above base speed range (ω_{sb} = 1.029 [p.u.] – FW region) the proposed method provides reference stator flux smaller than $1/\omega_m$. method. Therefore, the output torque capability of the IM is higher.

In Figure 9 simulation results under start up (with linear speed reference ramp), steady state at ω_m = 2.0 and m_L = 0.34 [p.u.] speed and braking cycle in both directions are shown. In this speed range, the operation results of two schemes are quite similar and no more differences in all state variable transients are observed.

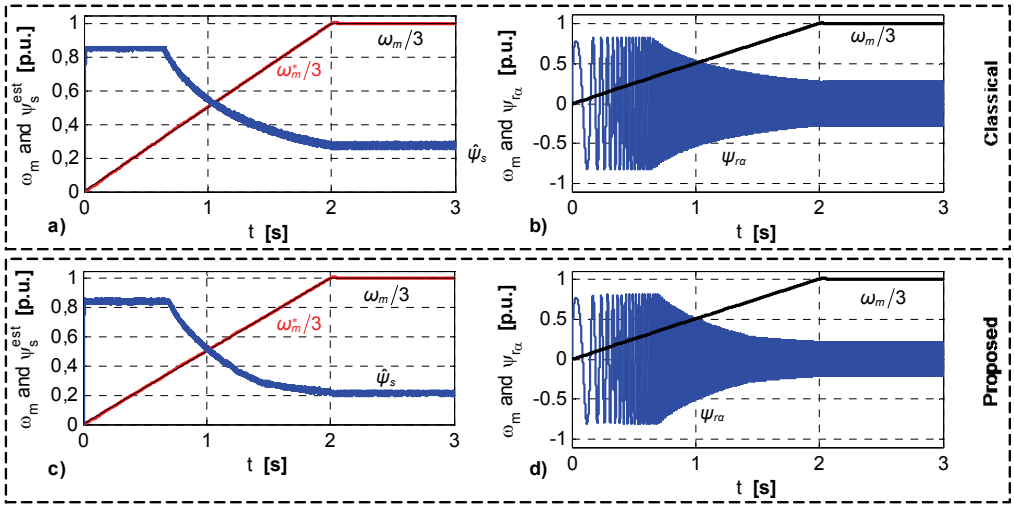

Fig. 8. No load start-up, steady state at ω_m = 3.0 [p.u.]:
(a, c) estimated stator flux, reference and motor speeds, (b, d) rotor flux and motor speeds

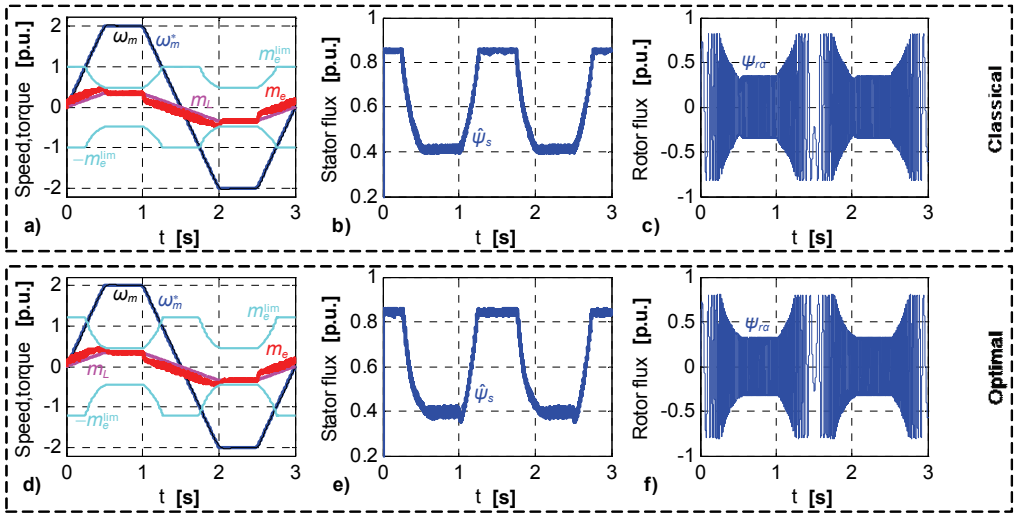

Fig. 9. Start up, steady state at ω_m = 2.0 [p.u.] speed and braking cycle in both directions for two FW methods: classical (a, b, c) and proposed (d, e, f); (a, d) reference and motor speeds, load, limit and motor torques, (b, e) estimated stator flux, (c, f) rotor flux

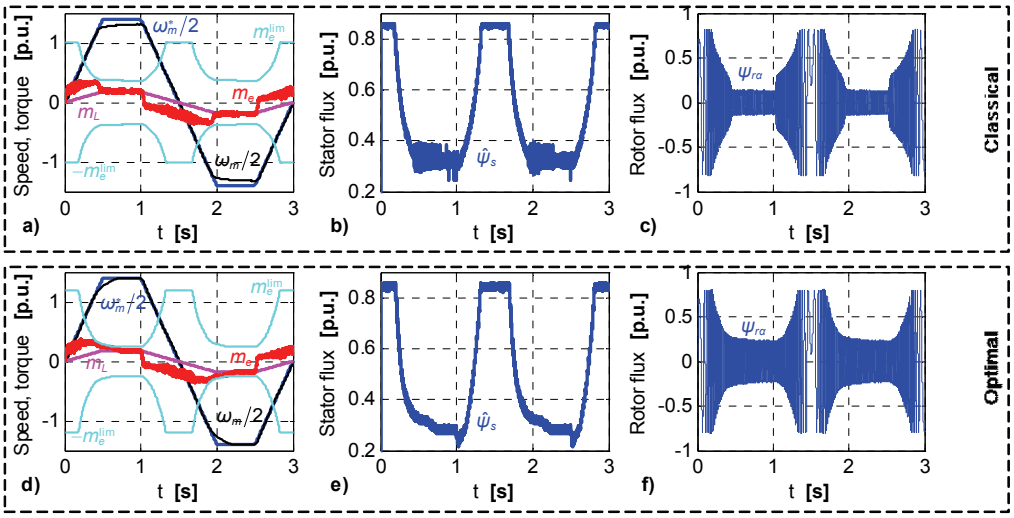

Fig. 10. Start up, steady state at $\omega_m = 2.8$ [p.u.] speed and braking cycle in both directions for two FW methods: classical (a, b, c) and proposed (d, e, f); (a, d) reference and motor speeds, load, limit and motor torques, (b, e) estimated stator flux, (c, f) rotor flux

In Figure 10 the similar results are shown, but for the maximal steady-state reference speed at $\omega_m = 2.8$ and $m_L = 0.18$ [p.u.]. In these operation conditions, we obtained some differences between the two control algorithms.

The classical scheme does not guarantee the stability due to the limited voltage conditions in the FW region II ($\omega_m > 2.47$ [p.u.]), therefore when load torque increases the rotor flux quickly decreases during the stator flux is kept in $1/\omega_m$ law. So the output torque is not enough for accelerating the speed, what we can see at the Fig. 10a, b, c.

On contrary, in the high speed region, the reference stator flux of the optimal scheme at a steady state (e.g., $t = 0.8$ s) is smaller than in the classical scheme (0.28 versus 0.32, see Fig. 10b, e), at the same time, the rotor flux is larger, which guarantees that electromagnetic torque is larger too (compare Fig. 10c, f), so it can give the speed acceleration to the reference value (see Fig. 10a, d).

6. CONCLUSION

For the field weakened operation of the induction motor drives a commonly used method is to vary the rotor flux reference in proportion to $1/\omega_m$. However in this method, because only the current limit is considered, the system cannot produce maximum torque, and is unstable in the high speed region.

In the contrary, the algorithm for FW with maintaining the voltage and current limits, guarantee the stable operation of the IM drive in the whole speed range. The algorithm presented in this paper enables to calculate the optimal flux reference for the SVM-DTC structure. This scheme to maintain the maximum torque capability of an IM over whole speed range included FW region is especially dedicated to drives operating in the wide speed region, as traction drives. In this scheme the base speed, maximum slip frequency and transition speed between two sub-regions of the FW, depending on the condition of the voltage and current limits, is automatically calculated, so smooth transition between speed regions is obtained.

The proposed scheme is compared with the classical method through simulations and it is verified that the new scheme provides the improved torque capability over the classical FW one.

REFERENCES

[1] BUJA G.S., KAŹMIERKOWSKI M.P., *Direct torque control of PWM inverter-fed AC motors – a survey*, IEEE Trans. Ind. Electron., Vol. 51, No. 4, 2004, pp. 776–784.

[2] CASADEI D., SERRA G., TANI A., *Constant frequency operation of a DTC induction motor drive for electric vehicle*, [in:] Proc. ICEM '96, Vol. 3, 1996, pp. 224–229.

[3] CASADEI D., SERRA G., TANI A., ZARRI L., *A robust method for flux weakening operation of DTC induction motor drive with on-line estimation of the break-down torque*, European Conf. on Power Electronics and Applications, EPE-2005, Dresden, pp. 10.

[4] CASADEI D., PROFUMO F., SERRA G., TANI A., *FOC and DTC: two viable schemes for induction motors torque control*, IEEE Trans. Power Electron., Vol. 17, No. 5, 2002, pp. 779–787.

[5] CASADEI D., SERRA G., STEFANI A., TANI A., ZARRI L., *DTC Drives for Wide Speed Range Applications Using a Robust Flux-Weakening Algorithm*, IEEE Trans. Ind. Electronics, Vol. 54, No. 5, 2007, pp. 2451–2461.

[6] DEPENBROCK M., *Direct self-control (DSC) of inverter-fed induction machine*, IEEE Trans. Power Electron., Vol. 3, 1988, pp. 420–429.

[7] KAŹMIERKOWSKI M.P., TUNIA H., *Automatic Control of Converter-Fed Drives*, Elsevier Amsterdam–London–New York–Tokyo, 1994.

[8] KAŹMIERKOWSKI M.P., WÓJCIK P., *Reliable Direct Torque Control with Flux Vector Modulation (DTC-FVM) for AC Motors*, IEEE International Symposium on Diagnostics for Electric Machines, Power Electronics and Drives, SDEMPED 2007, pp. 191–196.

[9] MARINO P., D'INCECCO M., VISCIANO N., *A comparison of direct torque control methodologies for induction motor*, IEEE Power Tech. Proceedings, Porto 2001, Vol. 2.

[10] MATIC P., RAKIĆ A., VUKOSAVIĆ S.N., *Induction motor torque control in field weakening regime by voltage angle control*, Proc. of the 14th Int. Power Electronics and Motion Control Conf. (EPE/PEMC), 2010, pp. T4-108–T4-115.

[11] MENGONI M., ZARRI L., TANI A., SERRA G., CASADEI D., *Stator Flux Vector Control of Induction Motor Drive in the Field Weakening Region*, IEEE Trans. on Power Electronics, Vol. 23, No. 2, 2008, pp. 941–949.

[12] NGUYEN THAC K., TARCHAŁA G., ORŁOWSKA-KOWALSKA T., *Comparative analysis of the chosen field-weakening methods for the Direct Rotor Flux Oriented Control drive system*, Archive of Electrical Engineering, Vol. 61, 2012 (in printing).

[13] ORŁOWSKA-KOWALSKA T., *Bezczujnikowe układy napędowe z silnikami indukcyjnymi*, Oficyna Wydawnicza Politechniki Wrocławskiej, Wrocław 2003.
[14] SIKORSKI A., KORZENIEWSKI M., RUSZCZYK A., KAŹMIERKOWSKI M.P., ANTONIEWICZ P., KOŁOMYJSKI W., JASIŃSKI M., *A comparison of properties of direct torque and flux control methods (DTC-SVM,DTC-δ, DTC-2x2, DTFC-3A)*, The Int. Conf. on "Computer as a Tool", EUROCON 2007, pp. 1733–1739.
[15] TAKAHASHI I., NOGUCHI T., *A New Quick-Response and High-Efficiency Control Strategy of an Induction Motor*, IEEE Trans. Ind. Applicat., Vol. IA-22, 1986, pp. 820–827.
[16] TRIPATHI A., KHAMBADKONE A.M., PANDA S.K., *Dynamic torque control performance of the Direct Flux Control scheme in field weakening range*, The 29th Annual Conf. of the IEEE Industrial Electronics Society, IECON '03, Vol. 1, 2003, pp. 220–225.
[17] TRIPATHI A., KHAMBADKONE A.M., PANDA S.K., *Dynamic control of torque in over-modulation and in the field weakening region*, IEEE Trans. on Power Electronics, Vol. 21, No. 4, 2006, pp. 1091–1098.
[18] WÓJCIK P., *Direct torque and flux control of inverter-fed induction motor drive including field weakening region*, Ph.D. Thesis, Warsaw University of technology, 2009.
[19] WÓJCIK P., *Flux Control with Space Vector Modulation (FC-SVM)*, The International Conf. on "Computer as a Tool" EUROCON, 2007, pp. 1759–1763.
[20] ZELECHOWSKI M., *Space Vector Modulated – Direct Torque Controlled (DTC-SVM) Inverter-Fed Induction Motor Drive*, Ph.D. Thesis, Warsaw 2005.